Nucleic Acids Research, 1993, Vol. 21, No. 4 887–896

Site-directed cross-linking studies on the *E.coli* tRNA-ribosome complex: determination of sites labelled with an aromatic azide attached to the variable loop or aminoacyl group of tRNA

Philip Mitchell, Katrin Stade, Monika Oßwald and Richard Brimacombe*
Max-Planck-Institut für Molekulare Genetik, Abteilung Wittmann, Ihnestraße 73, 1000-Berlin 33, Germany

Received November 19, 1992; Revised and Accepted December 21, 1992

ABSTRACT

tRNA^{Phe} from *E.coli*, modified with the photoreactive label N-(p-azidobenzoyl)-glycine (ABG) either at the naturally occurring nucleotide 3-(3-amino-3-carboxypropyl) uridine (acp^{3}U$_{47}$) or the α-amino group of Phe-tRNA^{Phe}, was bound nonenzymatically to 70S ribosomes in the presence of poly (U) or short synthetic mRNA molecules prepared by T7 transcription. The noncovalent complexes were subjected to a mild ultraviolet irradiation treatment and the sites of photo-incorporation were analysed. When the photo-affinity label was attached to the aminoacyl group cross-linking was observed from both A- and P-site bound tRNA and involved exclusively the 50S subunit. In both cases the major target of cross-linking was a single site in 23S RNA, localized to position A-2439. A lower yield of cross-linking to L27 from both P- and A-sites was also observed. In contrast, cross-linking from the acp^{3}U$_{47}$ derivative was specific for P-site bound tRNA and involved mainly (but not exclusively) the 50S subunit. In this case rRNA and ribsomal protein were labelled in approximately equal yields, the sites of cross-linking involving A-2309 in 23S RNA and L33. These results are discussed in the light of our present knowledge concerning the structural arrangement of the tRNA – ribosome complex.

INTRODUCTION

The application of photochemical cross-linking techniques has proved to be a useful approach to characterize the ribosomal binding sites of ligands such as rRNA, mRNA, or ribosomal antibiotics. Until now our own efforts in this field have been concentrated on the development of a 'site-directed cross-linking' strategy to delineate the topography of mRNA–ribosome interactions (1–3). In this approach complexes are formed between ribosomes and ligand analogues bearing one or more photoreactive groups at defined positions within their sequence. After photo-activation of the substituents by brief irradiation with light of a suitable wavelength the sites of cross-linking to rRNA or ribosomal protein are analysed. The detailed identification of sites of cross-linking within rRNA (especially at the nucleotide level) to defined positions within the ligand sequence provides very useful information, since these data correlate the topography of the ligand binding site with the three-dimensional arrangement of rRNA at the 'functional centre' of the ribosome. Taken together, the results obtained in our previous photo-affinity studies using mRNA analogues reveal serious errors in currently accepted models (4, 5) for the tertiary structure of 16S RNA, especially in the region of the molecule at the 'decoding centre' of the ribosome (for a detailed discussion, see ref. 3). These findings have prompted us to extend our application of the 'site-directed cross-linking' approach to incorporate studies using photoreactive analogues of tRNA and the nascent peptide, with the aim of obtaining an improved understanding of the topography of rRNA surrounding the mRNA:tRNA:peptide complex.

In our more recent studies using mRNA analogues (3) the photoreactive groups were s^{4}U residues, which can easily be incorporated into a desired RNA sequence by T_7 transcription of the correspoding synthetic DNA template. The results of chemical footprinting experiments (6–8) on the tRNA–ribosome complex suggest, however, that intimate contacts necessary for such 'zero-length' cross-linking between tRNA and rRNA exist only in the regions of the anticodon loop and the extreme 3′-terminus, and it is precisely these regions of the tRNA molecule for which cross-linking data of high resolution are already available (9, 10). In order to gain information conceming the topographical relationship between other portions of the tRNA molecule and rRNA we have therefore adopted the strategy developed by Ofengand and coworkers (11), involving the chemical attachment of a photoreactive probe to tRNA via a reactive group present in one of the naturally occuring modified nucleotides. The chemical reactivity of the α-amino or (in the case of lysyl–tRNA) ε-amino group of aminoacyl tRNA can be exploited in a similar manner, and previously a large number

* To whom correspondence should be addressed

of such photochemical cross-linking studies have aimed at defining structural correlates for the 'peptidyltransferase centre' of the ribosome (notably, refs. 12, 13). Moreover, the same approach can in principle be extended to investigate the path taken by the nascent peptide through the ribosome. Presently, the available data concerning the path of the peptidyl chain is largely limited to the results of gross morphological analyses and the conclusions reached are of two strongly contrasting viewpoints: thus, the question remains if the polypeptide leaves the ribosome in the vicinity of the peptidyltransferase centre (14), or rather passes through some kind of 'tunnel' and emerges at a topographically distant site (15, 16).

In this communication we report the first results of a systematic photo-affinity labelling study with the goal of defining in more detail the topography of the tRNA−ribosome complex and the path taken by the nascent peptide chain. $tRNA^{Phe}$ from *E.coli* or its aminoacylated derivative was chosen as a suitable substrate for derivatization with the N-hydroxysuccinimide ester of N-(p-azidobenzoyl)-glycine (ABG). Treatment of deacylated $tRNA^{Phe}$ with N-hydroxysuccinimide esters under controlled conditions (11) leads to the selective modification of the aliphatic primary amine of the 3-(3-amino-3-carboxypropyl) uridine (acp^3U) residue at position 47. This nucleotide is located in the variable loop of tRNA (which in the case of $tRNA^{Phe}$ is not extended) and therefore provides a suitable site of attachment for a probe in the central fold of the molecule. Under the same conditions the photolabel can also be attached to the α-amino group of Phe-$tRNA^{Phe}$. As noted above, in the latter case the aminoacyl tRNA analogue directly probes the region of the 'peptidyltransferase centre', and the experiment is technically very similar to the earlier report of Steiner *et al.* (13). However, for the purposes of our investigations this represents a simple model peptidyl tRNA and a starting point for mapping the route taken by the nascent polypeptide through the ribosome.

MATERIALS AND METHODS

Labelling and derivatization of $tRNA^{Phe}$

$tRNA^{Phe}$ from *E.coli* (Boehringer Mannheim) was dephosphorylated with alkaline phosphatase and 5′-labelled with γ-[^{32}P]ATP according to Gnirke *et al.* (17). 1 A_{260} unit of $tRNA^{Phe}$ was taken to be equivalent to 1500 pmol (17). Prior to labelling, full length tRNA was purified by electrophoresis, visualized by uv shadowing and recovered from the gel by extraction in the presence of phenol followed by ethanol precipitation. The labelled product was isolated either by electrophoresis in a 15% sequencing gel or by phenol extraction after dilution of the labelling mixture with 100 μl 0.1 M NaOAc pH 5.5, followed by two successive ethanol precipitations to remove excess [^{32}P]ATP. [^{3}H]Phe-$tRNA^{Phe}$ was prepared as described by Rheinberger *et al.* (18). Where appropriate, Phe-$tRNA^{Phe}$ was 5′-labelled with γ[^{32}P]ATP by the phosphate exchange reaction (as described in ref. 19) and recovered by phenol extraction and ethanol precipitation, as above. N-acetyl-Phe-$tRNA^{Phe}$ was prepared by treatment of Phe-$tRNA^{Phe}$ with acetic acid anhydride, as described by Haenni and Chapeville (20).

Derivatization of tRNA species with ABG N-hydroxysuccinimide ester (a kind gift from Dr H.Bäumert, University of Frankfurt) was performed according to the method of Podkowinski and Gornicki (21, cf. ref. 11). Monovalent derivatives of [^{3}H]Phe-$tRNA^{Phe}$, where the reagent was selectively coupled to either the acp^3U residue or the aminoacyl moiety, were obtained by performing the modification reaction prior to aminoacetylation or by acetylation of $tRNA^{Phe}$ (20) before aminoacylation and derivatization. Hereafter, derivatives of the acp^3U residue and the aminoacyl moiety are denoted by $tRNA^{Phe}$-ABG and ABG-Phe-$tRNA^{Phe}$, respectively. Following derivatization, ABG-Phe-$tRNA^{Phe}$ was purified by chromatography on benzoyl−DEAE cellulose columns, according to Steiner *et al.* (13).

Preparation of heteropolymeric mRNA molecules

The sequences of the two model mRNA molecules used in this study (written in the 5′ to 3′ direction) are given below. These transcripts were designed for other experimental objectives and for the purposes of these investigations it is only important to note that both contain unique codons for $tRNA^{Met}_f$ (AUG) and $tRNA^{Phe}$ (UUC) at adjacent positions within their sequences (indicated by underlining).

mRNA 1. GGG GGA CCA CCA AUG UUC AAA CCA CCC ACC UAC CCC ACU ACA U

mRNA 2. GGA GGA CAC UCU AUG UUC AAA GGA GGC GUG ACG GCG CGA GCA G

RNA molecules were prepared by T_7 transcription of synthetic DNA templates, as described previously (1). Transcription reactions were performed for 5 to 6 hours at 37°C. Full length transcripts were purified by gel electrophoresis (cf ref. 3) and recovered as above. Transcription yields were calculated spectrophotometrically, assuming an extinction coefficient of 2800 pmol/A_{260} unit. Transcript sequences were confirmed by reverse transcription sequencing reactions (see below) using a primer complementary to the 3′-terminal 17 nucleotides, or by oligonucleotide analysis of full length products isolated from analytical scale syntheses performed in the presence of α-[^{32}P]ATP or α-[^{32}P]UTP, using our standard procedures (22).

Formation of tRNA−ribosome complexes

Binding of 5′-[^{32}P]$tRNA^{Phe}$-ABG to the ribosomal P- and E-site. P-Site: For poly (U)-directed binding, 250 pmol 70S 'tight couple' ribosomes (18) were incubated with either 100 pmol or 500 pmol 5′-[^{32}P]$tRNA^{Phe}$-ABG in 500 μl of 50 mM Tris−HCl, pH 7.8, 10 mM $MgCl_2$, 160 mM NH_4Cl containing 0.2 mg/ml poly (U) for 15 min at 37°C. Binding in the presence of heteropolymeric mRNA molecules was performed either as above (at a 70S:mRNA ratio of 2:3), or using reconstituted 70S particles (3). In the latter case, 250 pmol 30S subunits were mixed with 400 pmol mRNA and 750 pmol 5′-[^{32}P]$tRNA^{Phe}$-ABG and incubated at 37°C for 15 min in 100 μl of buffer comprising 10 mM Tris−HCl, pH 7.8, 100 mM NH_4Cl, 10 mM $MgCl_2$. A stoichiometric amount of 50S subunits in the same buffer was then added and incubation continued for a further 15 min.

E-site: For preliminary P-site occupation, 125 pmol 70S ribosomes were incubated with 200 pmol N-acetyl-Phe-$tRNA^{Phe}$ in 125 μl of buffer comprising 50 mM Tris−HCl pH 7.8, 10 mM $MgCl_2$, 160 mM NH_4Cl, containing 0.2 mg/ml poly (U). 1000 pmol 5′-[^{32}P]$tRNA^{Phe}$-ABG in an equal volume of the above buffer were then added and incubation continued for 30 min at 37°C.

Binding of [^{3}H]Phe-$tRNA^{Phe}$-ABG to the ribosomal A-site. Initial P-site binding of $tRNA^{Met}_f$ (added in a ten-fold stoichiometric excess) in the presence of heteropolymeric mRNAs was performed using the 70S reconstitution system described above.

An equimolar amount of [^{3}H]Phe-tRNA^{Phe}-ABG was then added and the mixture made 15 mM in Mg^{2+}. Incubation was continued for a further 30 min at 37°C.

Poly (U) dependent binding of ABG-[^{3}H]Phe-tRNA^{Phe} to the ribosomal A- and P-site. Preparation of complexes between 70S ribosomes and ABG-[^{3}H]Phe-tRNA^{Phe} derivatives was performed essentially as described by Steiner *et al.* (13), except that the incubation buffer contained 20 mM HEPES−KOH pH 7.5 instead of Tris−HCl pH 7.5, and dithiothreitol was omitted. Where appropriate, 5′-[^{32}P]-labelled Phe-tRNA^{Phe} modified with the photolabel at both the acp^{3}U residue and the aminoacyl residue was bound to 70S ribosomes under the same conditions.

Irradiation of ribsomal complexes and analysis of cross-linked products

tRNA−ribosome complexes were subjected to ultraviolet irradiation for 2 or 3 minutes under our standard conditions (22). Control reactions were performed in parallel where the derivatized tRNAs were irradiated in binding buffer using the same procedure, prior to complex formation and subsequent irradiation. tRNA−ribosome complexes were separated from non-bound tRNA by a sucrose gradient centrifugation step (1) and recovered by ethanol precipitation.

Cross-linked ribosomal complexes were separated first into ribosomal subunits and then into rRNA and ribosomal protein fractions by two additional sucrose gradient centrifugation steps, at 0.3 mM Mg^{2+} and in 0.1% SDS, respectively (see Results, and ref. 1). Cross-linked ribosomal proteins were identified immunologically, as previously described (23). Assays were performed either on aliquots of the material recovered from the SDS gradients, or additionally (in the case of 5′-[^{32}P]tRNA^{Phe}-ABG cross-linked complexes) after purification of the individual complexes by electrophoresis in 8% polyacrylamide gels (cf. ref 2). Ribosomal protein complexes cross-linked to the aminoacyl moiety of ABG-[^{3}H]Phe-tRNA^{Phe} were digested to completion with RNase A and the proteins were preliminarily identified by electrophoresis (24) in the presence of total 50S ribosomal protein and selected marker ribosomal proteins. After detection of the non-labelled proteins by staining with 'Coomassie Blue', the band containing [^{3}H]Phe-labelled cross-linked protein was identified by fluorography using 'Amplify' (Amersham).

To identify sites on the rRNA, aliquots of the tRNA−rRNA cross-linked complexes were first digested with RNase H in the presence of selected pairs of oligodeoxynucleotides (25) and the products were analysed by gel electrophoresis in 5% polyacrylamide gels (1). ^{32}P-Labelled cross-linked tRNA−rRNA digestion products were detected by autoradiography, whereas gels containing ^{3}H-labelled samples were fixed by treatment with 10% acetic acid, 10% methanol and subjected to fluorography using Amplify. On the basis of the results obtained, 5′-[^{32}P]tRNA^{Phe}-ABG cross-linked complexes were separated from non-cross-linked rRNA by preparative RNase H digestions with suitable pairs of oligodeoxynucleotides and subsequent electrophoresis in polyacrylamide gels containing 7 M urea, 0.1% SDS (cf. ref. 3). The ^{32}P-labelled cross-linked complexes were detected by autoradiography, whereas the corresponding lower molecular weight non-cross-linked rRNA fragments (which served as controls in subsequent primer extension analyses) were detected by uv shadowing. For precise identification of the cross-link sites, primer extension reactions were performed on the isolated cross-linked complexes and the corresponding non-cross-linked control fragments using appropriate oligodeoxynucleotide primers, essentially as described by Kuechler *et al.* (26). Reactions were performed at 47°C for 45 min. tRNA−rRNA cross-linked complexes involving the aminoacyl moiety of ABG-[^{3}H]Phe-tRNA^{Phe} were observed to be unstable under the conditions of the RNase H digestion procedure (see Results) and therefore could not be separated from non-cross-linked rRNA: in these experiments primer extension reactions were carried out on aliquots of the tRNA−rRNA cross-linked complex/rRNA mixture and the products were compared with parallel reactions using rRNA isolated from controls with pre-irradiated tRNA derivatives. rRNA from the control samples in both types of experiment was used as substrate for parallel sequencing reactions (26).

RESULTS

The chemical structures of ABG N-hydroxysuccinimide ester and the corresponding tRNA^{Phe} derivatives (ABG-[^{3}H]Phe-tRNA^{Phe} and tRNA^{Phe}-ABG) used in these studies are given in Figure 1. The photoreactive azido group is positioned approximately 11Å and 17Å from the aminoacyl moiety and the uridinyl ring structure of acp^{3}U, respectively. ABG has an absorption maximum of ~275 nm, and is therefore not as sensitive to ambient light as substituted azidophenyl reagents. On the other hand, control experiments are required to differentiate between covalent complexes arising from photo-activation of the probe and concomitant inter- or intramolecular RNA cross-linking events. Preliminary experiments showed that irradiation of the reagent under the mild conditions employed in previous studies to analyse intramolecular RNA cross-links within ribosomal subunits (22) caused complete loss of the absorption peak at 275 nm within 3 minutes. Under such conditions, the amount of background cross-linking in ribosomal particles is minimized. To ensure that the cross-linked complexes analysed were dependent upon photo-activation of the label, control experiments using pre-irradiated tRNA derivatives were performed in parallel (see Figures 2 and 5, below). Furthermore, 'hidden' rRNA intramolecular cross-linking events which could possibly cause artefacts in the primer extension analyses could be discriminated by performing control extensions either on the corresponding non-

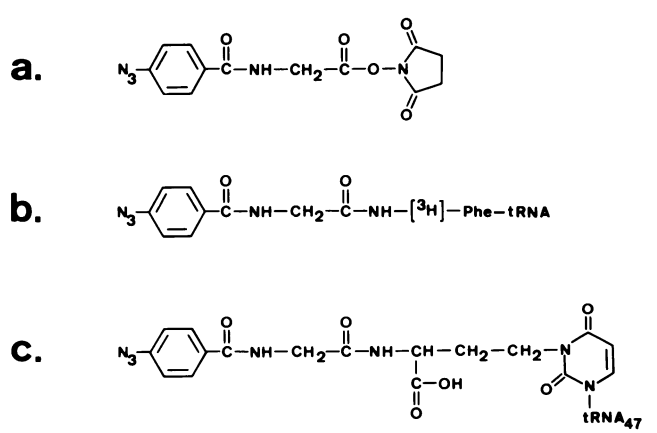

Figure 1. Chemical structures of *N*-(p-azidobenzyol)-glycine *N*-hydroxysuccinimide ester (**a**) and its derivative at the aminoacyl moiety of [^{3}H]PhetRNA^{Phe} (**b**) and the acp^{3}U residue at position 47 of tRNA^{Phe} (**c**).

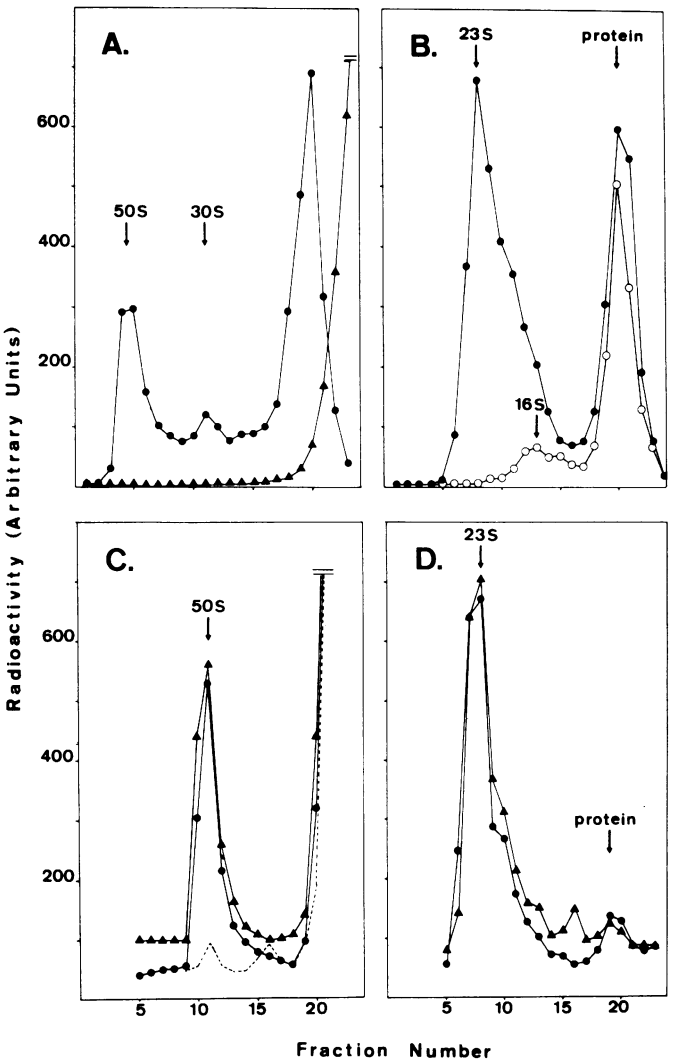

Figure 2. Sucrose gradient analyses of the products of cross-linking. Panels A and B are of $tRNA^{Phe}$ and Phe-$tRNA^{Phe}$ derivatized with ABG at position acp^3U_{47}, whereas C and D are of ABG-Phe-$tRNA^{Phe}$. In both cases the left-hand panels (A and C) are 'subunit' gradients (at low magnesium concentration), and the right-hand panels (B and D) are the corresponding SDS-containing gradients. Positions of 30S or 50S subunits (A and C), or of 16S RNA, 23S RNA and ribosomal proteins (B and D) are indicated. The direction of sedimentation is from right to left in all cases. In **Panel A** the filled triangles show the profile obtained for [^{3}H]Phe-$tRNA^{Phe}$-ABG bound at the A-site, the filled circles giving the corresponding profile for 5'-[^{32}P]$tRNA^{Phe}$-ABG at the P-site. **Panel B** shows the SDS gradients derived from the 50S peak (filled circles) and the 30S peak (open circles), respectively, from the latter gradient in panel A. In **Panel C**, results are shown for ABG-[^{3}H]Phe-$tRNA^{Phe}$ bound in the A-site (filled triangles) or the P-site (filled circles), respectively, and the dotted line is the result of a P-site bound pre-irradiated control experiment. **Panel D** gives the corresponding SDS gradients from the A-site (filled triangles) and P-site (filled circles) samples, derived from the 50S peaks in panel C. The amount of radioactivity present in each fraction is indicated in arbitrary units to allow direct comparison of the individual profiles. The gradients shown in panel A were run longer than the corresponding gradients in panel C to increase the resolution of the subunits.

complexed rRNA fragments (in the case of experiments with 5'-[^{32}P]$tRNA^{Phe}$-ABG) or on rRNA isolated from samples comprising pre-irradiated tRNA derivatives (in the analyses of ABG-[^{3}H]Phe-$tRNA^{Phe}$ samples).

$tRNA^{Phe}$ derivatives carrying the photolabel ABG attached to position acp^3U_{47} or to the aminoacyl moiety were bound non-enzymatically to 70S ribosomes under experimentally defined conditions (13, 18) which allow preferential occupation of the ribosomal A-, P- or E-site (see Materials and Methods). Ribosomal complexes were subjected to brief irradiation with ultraviolet light and then separated into rRNA and ribosomal protein fractions by a series of sucrose gradient centrifugation steps. Covalent complexes involving tRNA cross-linked to rRNA were characterized by RNase H analyses and primer extension; cross-linked ribosomal proteins were determined by a combination of gel electrophoresis and immunological identification, respectively. The patterns of cross-linked products obtained when the derivatized tRNA species were preferentially bound to either the ribosomal A-, P-, or E-site were compared: both acp^3U- and aminoacyl-derivatized tRNAs gave unique patterns of cross-linking which could be assigned to the P-site, and to both the P- and A-sites, respectively (see Figures 2 and 5, below). Details are given below for analyses of $tRNA^{Phe}$-ABG bound to the P-site in the presence of mRNA 1 (see Materials and Methods) using the 70S reconstitution system of Dontsova *et al.* (3), and for ABG-Phe-$tRNA^{Phe}$ bound in the P- and A-site of 70S 'tight couples' in a poly (U) dependent manner; identical results were obtained with $tRNA^{Phe}$-ABG when reconstituted or 'tight couple' 70S ribosomes were employed and were independent of the type of mRNA used (poly (U) or synthetic transcripts).

Examples of sucrose gradient analyses of irradiated tRNA−ribosome complexes containing P- and A-site bound tRNA species derivatized at position acp^3U_{47} or the aminoacyl moiety are shown in Figure 2 (upper and lower panels, respectively). The amount of radioactivity present in each fraction is indicated in arbitrary units to allow direct comparison of the individual profiles in each panel. At 0.3 mM Mg^{2+} the 70S complexes are dissociated into 50S and 30S subunits, non-cross-linked tRNA remaining in the upper fractions of the gradient (panels A and C). Subsequent centrifugation in gradients containing 0.1% SDS (panels B and D) separates the ribosomal subunits into fractions containing rRNA or ribosomal protein. Cross-linking from position 47 is observed to be specific for P-site bound tRNA (see panel A), the major target being the 50S subunit. The yield of cross-linking to the large subunit (estimated as the fraction of radioactivity originally bound to 70S which comigrated with the 50S peak upon subsequent gradient analysis at 0.3 mM Mg^{2+}) was approximately 10%. SDS gradient analysis of the labelled 50S peak shows approximately equal incorporation of label into the 23S RNA and ribosomal protein fractions, whereas the much lower level of cross-linking to the 30S subunit is predominantly to ribosomal protein (panel B). In the absence of mRNA an identical cross-linking pattern was observed but at an approximately five-fold decrease in yield (consistent with cross-linking occurring from the P-site, cf. ref. 18). Furthermore, the pattern of cross-linking was independent of the ratio of 70S to $tRNA^{Phe}$-ABG (within the range 5:2 to 1:2) used in the binding reaction. Experiments where $tRNA^{Phe}$-ABG was directed to the E-site revealed low levels of the same cross-linked products (data not shown), which we attribute to background P-site occupation. Confirmation that the observed cross-linking occurs in the P-site and not the E-site was provided in experiments with Phe-$tRNA^{Phe}$ modified at both the acp^3U residue and the aminoacyl moiety (see below): in this case binding to the E-site is excluded. In contrast to the cross-linking pattern for acp^3U_{47} derivatives, attachment of the label to the aminoacyl moiety yields patterns which are almost identical for both A- and

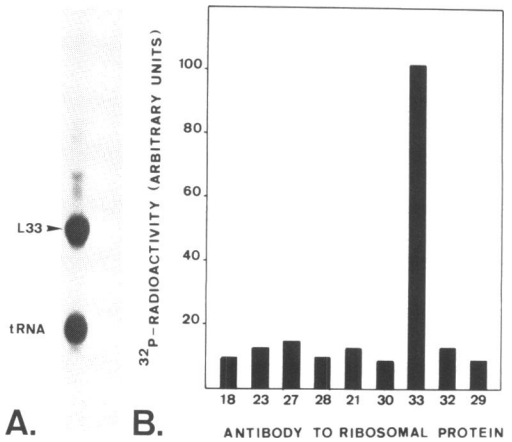

Figure 3. Combined electrophoretic and immunological analysis of ribosomal protein cross-linked to 5′-[^{32}P]tRNA^{Phe}-ABG. **Panel A**: Separation of tRNA−protein cross-linked complexes in an 8% polyacrylamide gel. The direction of electrophoresis was from top to bottom. **Panel B**: Results of an immunoassay performed on non-purified cross-linked material using a series of immunosera specific for individual 50S ribosomal proteins. Since the test is a qualitative rather than quantitative assay, the amount of radioactivity bound by each antibody is indicated in arbitrary units.

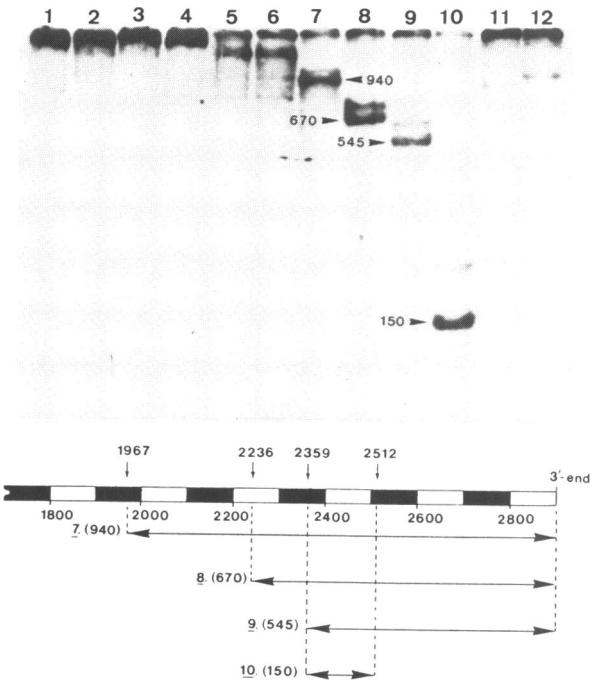

Figure 4. Preliminary localization of the site of cross-linking between P-site bound ABG-[^{3}H]Phe-tRNA^{Phe} and 23S RNA by the RNase H method. The upper portion of the Figure shows a fluorograph obtained upon electrophoretic analysis of the digestion products. Digestions were performed in the presence of pairs of deoxyoligonucleotides complementary to sequences centred at positions 250/495 (lane 1), 495/780 (lane 2), 780/1045 (lane 3), 1045/1366 (lane 4), 1366/1626 (lane 5), 1626/1737 (lane 6), 1737/1967 (lane 7), 1967/2236 (lane 8), 2236/2359 (lane 9), 2359/2512 (lane 10), 2512/2624 (lane 11) and 2624/2823 (lane 12). ^{3}H-labelled (cross-linked) fragments visible in the fluorograph are indicated by arrows and their expected lengths are shown. The locations of these fragments within the 23S RNA are depicted schematically in the lower portion of the Figure. Only in lane 10 is the selectively excised (low molecular weight) fragment ^{3}H-labelled, clearly localizing the site of cross-linking to this portion of 23S RNA (positions 2359 to 2512).

P-site bound tRNAs (panel C). Cross-linking is observed only to the 50S subunit (panel C) and involves almost exclusively 23S RNA. (panel D). The yield of cross-linking in this case was approximately 25% for both A- and P-site bound tRNA. Included in panel C is the profile from an irradiated complex formed with a control pre-irradiated (P-site bound) tRNA derivative. It can be seen that irradiation of the tRNA derivative prior to complex formation yields greatly reduced levels of cross-linking to both subunits (the corresponding control for A-site bound tRNA gave a similar low level of cross-linking).

The identities of the cross-linked ribosomal proteins were determined by the immuno-affinity assay of Gulle *et al.* (23). Assays were performed either directly on material recovered from the SDS-containing gradient peaks or on individual cross-linked complexes after purification by gel electrophoresis (cf. ref. 2). Since the results of the immuno-affinity assay cannot be interpreted quantitatively (27), a combination of immunological and electrophoretic analyses provides a clearer impression of the relative amounts of individual cross-linked products.

Figure 3 shows a representative example of such a combined analysis of the 50S subunit peak labelled with P-site bound 5′[^{32}P]tRNA^{Phe}-ABG (cf. panel B of Figure 2). Gel electrophoresis reveals a single major cross-linked complex (panel A), together with residual non-cross-linked tRNA. Immuno-affinity assays were performed on the non-purified material using a range of antibodies specific to 50S ribosomal proteins of appropriate molecular weight, as inferred from the electrophoretic mobility of the cross-linked complex. The data obtained (panel B) clearly identify L33 as the cross-linked protein and this result was subsequently confirmed by immuno-affinity analysis of the gel-purified complex. Similarly, a single product was also observed upon electrophoretic analysis of complexes involving ABG[^{3}H]Phe-tRNA^{Phe} cross-linked to ribosomal protein and which co-migrated with a group a proteins consisting of L18, L23 and L27. Subsequent immuno-affinity analysis provided an unambiguous identification of L27 (data not shown). 30S ribosomal protein cross-linked to 5′[^{32}P]tRNA^{Phe}-ABG (cf. Figure 2B) could not be identified unambiguously by the immunological method.

Sites of cross-linking within rRNA were analysed using the two-step procedure described by Rinke-Appel *et al.* (2). The cross-linked nucleotide was initially localized to a region within the rRNA sequence by a screening procedure involving the release of sub-fragments of the molecule by addressed cleavage with RNase H and subsequent gel electrophoretic analysis of the digestion products. The precise sites of cross-linking were then determined by primer extension analysis. An example of the RNase H method is given in Figure 4; primer extension analyses are shown in Figure 5.

In the RNase H method, aliquots of the rRNA cross-linked complexes are digested with the enzyme in the presence of selected deoxyoligonucleotides complementary to sites within the rRNA sequence separated by ~50−300 nucleotides. By performing a series of such digestions with pairs of DNA oligomers, the complete molecule can be 'screened' as a collection of excised sub-fragments. Since in these experiments the cross-linked ligand is radiolabelled, a band of high electrophoretic mobility is detected on the autoradiograph or fluorograph of the gel only if the site of cross-linking lies within the selectively excised fragment. Once the site(s) of cross-linking

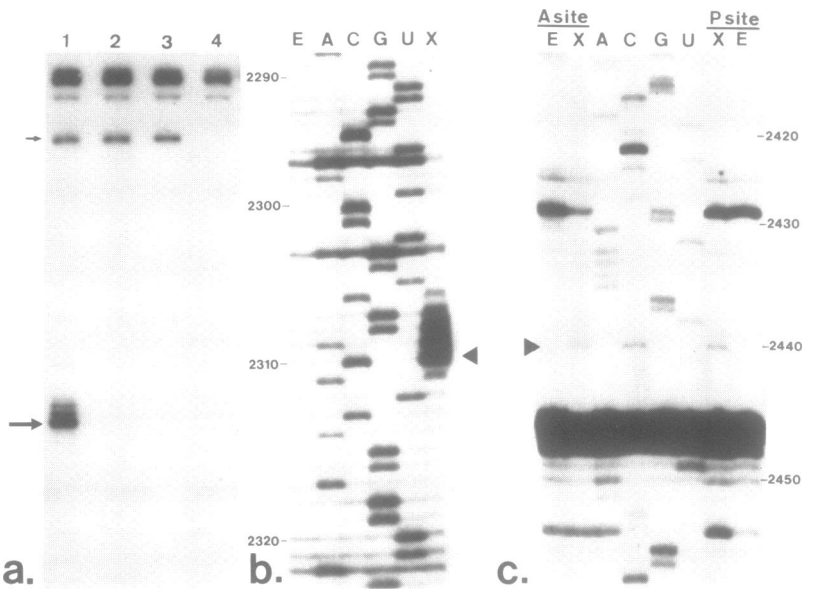

Figure 5. Primer extension analyses of 23S RNA cross-linked complexes. **Panel a**: Extension analysis showing reagent-dependent stop in complexes involving $tRNA^{Phe}$-ABG. lane 1, $tRNA^{Phe}$-ABG; lane 2, $tRNA^{Phe}$; lane 3, pre-irradiated $tRNA^{Phe}$-ABG; lane 4, control 23S RNA fragment. The reagent-dependent stop is indicated by a large arrow on the left-hand side of the panel (a reagent-independent stop which gave rise to background levels of cross-linking in the control samples, as well as in the derivatized tRNA sample, is indicated by a small arrow). **Panel b**: Localization of the site of cross-linking to $tRNA^{Phe}$-ABG in the 23S RNA. A, C, G, and U are dideoxy sequencing lanes. X indicates the primer extension lane of the cross-linked sample, E denotes that of the 23S RNA control fragment (cf. lanes 1 and 4 of panel a, respectively). The major stop observed in the cross-linked sample at position 2310 is indicated by an arrowhead. **Panel c**: Corresponding extension analyses of cross-linked samples involving ABG-PhetRNA^{Phe}. Extension reactions were performed on non-digested cross-linked 23S RNA (X) and on 23S RNA obtained from pre-irradiated controls (E) for both A- and P-site probing experiments. A specific stop in the cross-linked sample lane is observed at position 2440 in both A- and P-site probes (indicated with an arrowhead, as in panel b).

have been localized to a specific region of the rRNA in this manner, subsequent rounds of digestions are performed to refine the analysis as much as possible.

The example given in Figure 4 shows a scan of 23S RNA cross-linked to ABG-[^{3}H]Phe-$tRNA^{Phe}$. In this particular example cross-linking was performed in a P-site probing experiment (cf. panel D of Figure 2), although the gel patterns observed were identical for both P- and A-site bound tRNAs. It can be seen that the cross-link lies within a region of the 23S RNA approximately 150 nucleotides in length (lane 10), comprising positions ~2359–2512, the sites in the rRNA being given as the central positions of the sequence complementary to the deoxyoligonucleotides used in individual digestions. The labelled fragments of considerably higher molecular weight visible in lanes 7–9 can be assigned to the portion of 23S RNA extending from the excised region to the 3′-terminus; those observed in lanes 5 and 6 are too large (well over 1000 nucleotides in length) to provide useful information on the site of cross-linking. The radiolabelled excised fragments are detected as doublets on the fluorograph: this effect was observed to be characteristic for ABG-[^{3}H]aminoacyl tRNAs and is presumably due to partial hydrolysis of the aminoacyl ester linkage under the conditions of the RNase H digestion procedure.

Similar gel analyses were performed on rRNA cross-linked samples involving 5′-[^{32}P]$tRNA^{Phe}$-ABG. As with ABG-Phe-$tRNA^{Phe}$, cross-linking to 23S RNA from acp^3U_{47} was confined to a single region located towards the 3′-terminus of the molecule but in this case to a different sub-fragment, namely comprising positions ~2277 to 2363 (data not shown). Analyses of the 16S RNA cross-linked complexes gave more complicated patterns, involving several regions of the rRNA. Due to the intrinsically low yield of cross-linking to 16S RNA (see Figure 2, panel B) and the observed heterogeneity of the cross-linked products, these sites of cross-linking were not investigated further.

The precise sites of cross-linking within the 23S RNA were determined by primer extension analysis, using the method of Kuechler *et al.* (26). This technique is based on the observation that reverse transcriptase pauses or stops at sites of modification in the RNA template (28, 29). Analyses were performed using primers complementary to sequences outside of the region containing the cross-link site, as defined by the RNase H data. Sites of cross-linking were inferred as involving the nucleotide immediately after those pauses in the extension reactions which were reproducibly observed at a significantly higher intensity on the autoradiographs than the corresponding sites in the control lanes, and which were entirely consistent with the results of the RNase H method.

Figure 5 shows primer extension analyses for sites of cross-linking from both acp^3U_{47} and aminoacyl-derivatized samples. In the case of the $tRNA^{Phe}$-ABG cross-link, the substrate for primer extension is a 23S RNA fragment released upon RNase H digestion and separated from the equivalent non-cross-linked material by gel electrophoresis, the latter providing an internal control. Similar preparative RNase H digestions performed upon non-derivatized $tRNA^{Phe}$ and on pre-irradiated $tRNA^{Phe}$-ABG complexes revealed much reduced levels of cross-linking in this region of 23S RNA and extension reactions on these samples are included in the analysis. In experiments where the photolabel was attached to the aminoacyl moiety (panel c), extension reactions were performed directly on material isolated from the

gradient fractions (due to the instability of the the aminoacyl ester linkage noted above) and compared with parallel extensions using 23S RNA from pre-irradiated control samples.

Panel a compares the extension products obtained from $tRNA^{Phe}$-ABG with those of non-derivatized and pre-irradiated controls (lanes 1−3, respectively) and with the corresponding non-cross-linked control 23S RNA fragment (lane 4). A strong signal is observed which is dependent upon the reagent and which is abolished by pre-irradiation of the derivatized tRNA. This pause is centred at position 2310 in the 23S RNA sequence (panel b), corresponding to a site of cross-linking at A-2309. The adjacent bands at positions 2306−2309 may represent a microheterogeneity at the site of cross-linking, or may be a result of 'stuttering' of the enzyme. The analysis also reveals a discrete site of photo-incorporation which is independent of the cross-linking reagent (indicated by a small arrow in panel a) and which could be localized to position U-2259 (data not shown). The usefulness of this latter data is, however, limited since the position of cross-linking within the tRNA cannot be inferred.

A single characteristic band was detected in analyses of aminoacyl-derivatized samples for both A- and P-site bound tRNA. The stop at position 2440 observed with ABG-[^{3}H]Phe-$tRNA^{Phe}$ cross-links (panel c) is considerably weaker than that seen in the acp^3U_{47} derivative extension reactions (panels a and b), primarily due to the fact that in this case the analysis was performed on the mixture of tRNA−rRNA cross-linked complex and non-cross-linked rRNA, as opposed to an isolated cross-linked product. Both cross-link site analyses were entirely reproducible (the strong pause beneath the cross-link site in both cross-link and control samples in panel c is due to the presence of an m^2G residue (30, cf. ref. 29)). In the autoradiograph shown an apparently cross-link-specific stop is observed at position A-2453 for P-site bound ABG-[^{3}H]Phe-$tRNA^{Phe}$ (cf. ref. 13). However, this result was not reproducibly observed with our reagent and therefore is not considered as a definitive cross-link site analysis in this case. The observation of identical cross-linked products for P- and A-site bound ABG-[^{3}H]Phe-$tRNA^{Phe}$ is not inconsistent, given the close proximity of the 3′-termini of tRNA bound in the P- and A-sites and the length and flexibility of the photolabel. Confirmation that cross-linking to A-2439 occurs both from the P- and A-sites was obtained by primer extension reactions performed on cross-linked samples of Phe-$tRNA^{Phe}$ modified both at acp^3U and the aminoacyl moiety: stops were observed corresponding to cross-linking at A-2439 in both A- and P-site bound tRNA, whereas the cross-link at A-2309 was detected only for the P-site bound derivative.

DISCUSSION

A series of complexes comprising photoreactive tRNA derivatives, model mRNA molecules and ribosomes were formed *in vitro* under established conditions which allow preferential occupation of the A-, P- or E-site. Specific cross-links were observed when the label was attached to either position 47 or the aminoacyl moiety. These cross-links could be assigned to particular ribosomal binding sites by comparing the results obtained with the various (A-, P- or E-site) ribosomal complexes investigated. Since the yield of each individual cross-linked product represents only a minor fraction of the total ribosomal bound tRNA, such a qualitative assessment avoids a possible false assignment of an observed cross-link to the principal binding site due to a 'high yield' cross-linking event at another site where a lower level of binding has occured. On the basis of this comparative assessment, we attribute cross-links to A-2309 of 23S RNA and L33 from acp^3U_{47} to P-site bound tRNA, and cross-links to A-2439 of 23S RNA and L27 from the aminoacyl moiety to both A- and P-site bound tRNA.

Data from previous studies concerning the location of the central fold of tRNA on the ribosome are largely limited to the identification of cross-linked ribosomal proteins (e.g. ref. 31). These data agree with the known gross morphological localization of the ribosomal tRNA binding sites (see refs. 10, 32), but the limited resolution conceming the structural arrangement of individual proteins in the ribosome and the lack of detailed knowledge of the sites of cross-linking (at the amino acid level) involved severely limit the interpretation of the results in terms of the mutual arrangement of the A- and P-sites. These same limitations apply to the model proposed by Ofengand and coworkers (33), based on their cross-links to S19 from positions s^4U_8 and acp^3U_{47} of $tRNA^{Phe}$ bound in the A- and P-sites, respectively, as well as to the large body of other RNA−protein cross-linking data available. For these reasons we believe that more detailed models of the structural organization of the tRNA−ribosome complex will neccessitate further data correlating the alignment of tRNA (and mRNA) with the three-dimensional arrangement of rRNA, rather than the spatial arrangement of the ribosomal proteins. The results presented in these studies, together with other data which correlate the mutual arrangement of tRNA and 23S RNA, are summarized in Figure 6.

Notably, in the same communication mentioned above (33) Ofengand's laboratory reported a significant level of cross-linking from acp^3U_{47} of P-site bound $tRNA^{Phe}$ to 23S RNA using an azidonitrophenyl photolabel of similar length to ABG, yet were unable to characterize the site(s) of cross-linking. The most pertinent study to date in this respect is that of Podkowinski and Gomicki (21), who analysed the location of the 'D' loop of P-site bound tRNA on the ribosome using affinity labels attached to position 20:a of $tRNA^{Met}_m$ from lupin. In addition to cross-linking to proteins S7, L33 and L1, these authors reported significant cross-linking with an 18−19 Å long probe to both 16S and 23S RNA, the site in the latter being localized to a fragment comprising positions 2281 to 2358. Position 20:a (corresponding to an insertion between positions 20 and 21 in the structure of $tRNA^{Phe}$) is located in the central fold of tRNA but on the opposite side of the molecule with respect to position 47. Thus, there is good agreement between the results of Podkowinski and Gomicki (21) and of these studies concerning the location of the central fold of tRNA in the ribosomal P-site: position A-2309 in 23S RNA lies within the fragment containing the site(s) of cross-linking to position 20:a and, furthermore, L33 was the major protein labelled from both sites. Our results provide the first detailed localization of a site of cross-linking within rRNA from the central fold of tRNA. Thus, the position of P-site bound tRNA can now be directly correlated with the arrangement of rRNA at three different positions; viz nucleotide 34 to position C-1400 in 16S RNA (9), nucleotide 76 to position G-1945 in 23S RNA (10) and nucleotide 47 to position A-2309 in 23S RNA (these studies), corresponding to the anticodon loop, the 3′-terminus and the central fold of the molecule, respectively.

In contrast, the pattem of cross-linking observed when the affinity label was attached to the aminoacyl moiety was identical for both P- and A-site bound tRNA and involved position A-2439

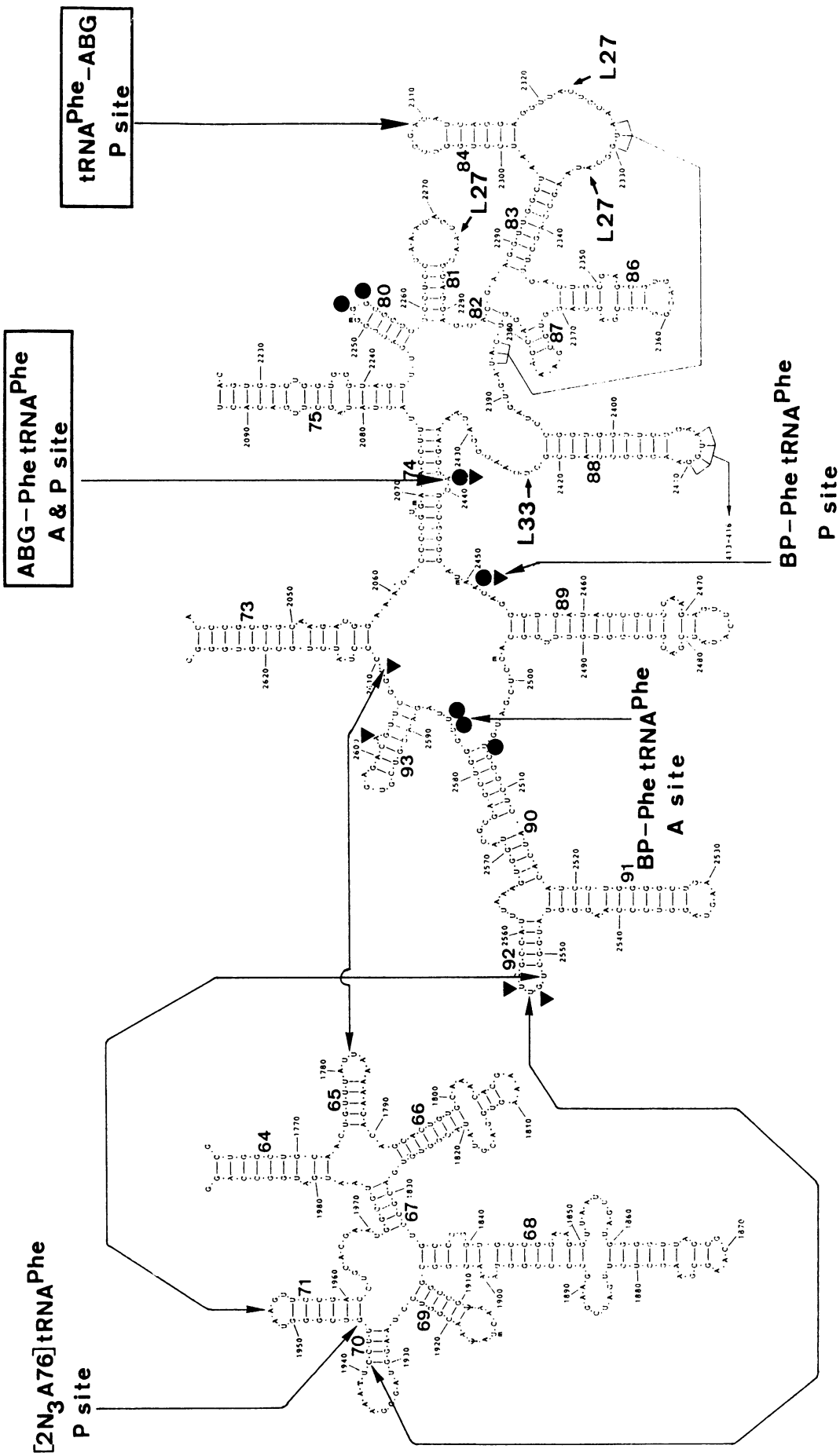

Figure 6. Secondary structure of helices 64–71 and 73–75/80–93 of 23S RNA, showing topographical data concerning tRNA–ribosome interactions. Sites of cross-linking between 23S RNA and tRNA (refs. 10 and 13, and these studies) are denoted by arrows and the nature of the photoreactive derivatives, together with the defined ribosomal binding site in each case, are indicated (those analysed in these studies are boxed). Sites protected from chemical modification by features of the 3′-end of tRNA bound in the A- or P-site (6, 8) are denoted by small triangles or circles, respectively. Also included in the Figure are data from intramolecular cross-linking studies (25) (denoted by double-headed arrows) which define interactions between these two regions of the secondary structure, together with sites of cross-linking to ribosomal proteins L27 and L33 (27).

in 23S RNA and L27. A-2439 is situated in helix 74 (see Figure 6), which together with helices 73, 89, 90 and 93 form a ring structure that has been consistently associated with peptidyltransferase activity (8, and references within). The most convincing evidence for a congruent location of the peptidyltransferase activity and this feature of the 23S RNA secondary structure is provided by previous cross-linking experiments using a benzophenone derivative of Phe-tRNA^{Phe} (BP-Phe-tRNA^{Phe}) as a photo-affinity probe (12, 13). Cross-linking with this reagent was observed at positions 2451/2452 and 2484/2485 in 23S RNA when the modified tRNA was positioned in the P- and A-site, respectively (see Figure 6). Furthermore, Noller's group have identified a catalogue of bases in rRNA which are involved either directly or indirectly in ribosomal interactions with rRNA (6–8) and their results suggest that interactions between tRNA and 23S RNA are predominantly mediated via the aminoacyl extremity of tRNA (8). Those A- and P-site protections in 23S RNA which are attributed to the 3′-end of tRNA are also included in Figure 6.

Nucleotides in the vicinity of the 3′-terminus of tRNA bound in the P- or A-site must lie at, or close to, the peptidyltransferase centre of the 50S subunit. A good agreement exists between the structural correlates for the peptidyltransferase centre identified by the chemical protection studies noted above (8) and the results of photo-affinity labelling experiments (12, 13, and these studies). Thus, three of the four nucleotides labelled by BP-Phe-tRNA^{Phe} (13) are also protected from chemical modification. Similarly, the site of cross-linking to ABG-Phe-tRNA^{Phe} (A-2439) corresponds to an acyl group dependent protection for A- and P-site bound tRNA (8). Additional chemical protections were also observed at positions G-2252, G-2553 and U-2506 for P-site bound tRNA, and at G-2553, ψ-2555, A-2602 and U-2609 for A-site bound tRNA. Moazed and Noller previously reported protection of A-1916, A-1918 and U-1926 by P-site bound tRNA (6) which they since attribute primarily to 30S–50S subunit interactions (8). Nevertheless, sites within this region of 23S RNA are clearly juxtaposed with the set of nucleotides noted above, as evidenced by direct intramolecular cross-links between positions U-1782 and G-2608/U-2609, and between the loop-ends of helices 70, 71 and 92 (25) (see Figure 6). Moreover, as already noted 2-azidoadenosine incorporated at position 76 of tRNA^{Phe} or *N*-acetyl-Phe-tRNA^{Phe} has been cross-linked from the P-site to position G-1945 of 23S RNA (10). The latter study also reported concomitant cross-linking to L27, the same protein labelled with ABG-Phe-tRNA^{Phe} in these studies. L27 has been cross-linked to three sites in 23S RNA (positions 2272–2283; 2320–2323 and 2332–2337) (27) which, due to the tertiary interaction between positions 2328–2330 and 2385–2387 (34), are juxtaposed in the three-dimensional arrangement of 23S RNA at a site congruent with the ring structure connecting helices 74, 75, 80–82 and 88 (see Figure 6).

Thus, all these regions of the 23S RNA must therefore be arranged in an intricate manner at the peptidyltransferase centre. By using peptidyl tRNA analogues with the photoreactive group incorporated at incremental distances from the 3′-terminal A residue of tRNA (cf. ref. 35), the application of photo-affinity labelling techniques described in this communication has the potential to define more precisely the spatial arrangment of these interrelated sites. In a similar manner, cross-linking from sites within the anticodon loop of tRNA, in conjunction with data from mRNA analogues containing photoreactive nucleotides within, or close to, the P- and A-site codons, should provide a more detailed picture of the tertiary structure of 16S RNA at the decoding region. Studies of the latter type are already well underway, and the results will be published in due course.

ACKNOWLEDGEMENTS

We are most grateful to Dr Hans Bäumert for supplying the photoreactive reagent and to Dr Knud Nierhaus for his advice on tRNA acylation and complex formation. The work was supported in part by a grant from the Deutsche Forschungsgemeinschaft (SFB 9).

REFERENCES

1. Stade,K., Rinke-Appel,J. and Brimacombe,R. (1989) *Nucleic Acids Res.* **17**, 9889–9908.
2. Rinke-Appel,J., Jünke,N., Stade,K. and Brimacombe,R. (1991) *EMBO J.* **10**, 2195–2202.
3. Dontsova,O., Dokudovskaya,S., Kopylov,A., Bogdanov,A., Rinke-Appel,J., Jünke,N. and Brimacombe,R. (1992) *EMBO J.* **8**, 3105–3116.
4. Brimacombe,R., Atmadja,J., Stiege,W. and Schüler,D. (1988) *J. Mol. Biol.* **199**, 115–136.
5. Stern,S., Weiser,B. and Noller,H.F. (1988) *J. Mol. Biol.* **204**, 447–481.
6. Moazed,D. and Noller,H.F. (1989) *Cell* **57**, 585–597.
7. Moazed,D. and Noller,H.F. (1990) *J. Mol. Biol.* **211**, 135–145.
8. Moazed,D. and Noller,H.F. (1991) *Proc. Natl. Acad. Sci. USA* **88**, 3725–3728.
9. Prince,J.B., Taylor,B.H., Thurlow,D.L., Ofengand,J. and Zimmermann, R.A. (1982) *Proc. Natl. Acad. Sci. USA* **79**, 5450–5454.
10. Wower,J., Hixson,S.S. and Zimmermann,R.A. (1989) *Proc. Natl. Acad. Sci. USA* **86**, 5232–5236.
11. Ofengand,J., Schwartz,I., Chinali,G., Hixson,S.S. and Hixson,S.H. (1977) *Methods Enzymol.* **46**, 683–702.
12. Barta,A., Steiner,G., Brosius,J., Noller,H.F. and Kuechler,E. (1984) *Proc. Natl. Acad. Sci. USA* **81**, 3607–3611.
13. Steiner,G., Kuechler,E. and Barta,A. (1988) *EMBO J.* **7**, 3949–3955.
14. Ryabova,L.A., Selivanova,O.M., Baranov,V.I., Vasiliev,V.D. and Spirin,A.S. (1988) *FEBS Lett.* **226**, 255–260.
15. Bernabeu,C. and Lake,J.A. (1982) *Proc. Natl. Acad. Sci. USA* **79**, 3111–3115.
16. Yonath,A., Leonard,K.R. and Wittmann,H.G. (1987) *Science* **236**, 813–816.
17. Gnirke,A., Geigenmüller,U., Rheinberger,H.-J. and Nierhaus,K.H. (1989) *J. Biol. Chem.* **264**, 7291–7301.
18. Rheinberger,H.-J., Geigenmüller,U., Wedde,M. and Nierhaus,K.H. (1988) *Methods Enzymol.* **164**, 658–670.
19. Chen,J.-K., Franke,L.A., Hixson,S.S. and Zimmermann,R.A. (1985) *Biochemistry* **24**, 4777–4784.
20. Haenni,A.-L. and Chapeville,F. (1966) *Biochim. Biophys. Acta* **114**, 135–148.
21. Podkowinski,J. and Gomicki,P. (1991) *Nucleic Acids Res.* **19**, 801–808.
22. Brimacombe,R., Greuer,B., Gulle,H., Kosack,M., Mitchell,P., Oβwald,M., Stade,K. and Stiege,W. (1990) In Spedding,G. (ed.) *Ribosomes and Protein Synthesis. A Practical Approach.* IRL Press, Oxford, pp. 131–159.
23. Gulle,H., Hoppe,E., Osswald,M., Brimacombe,R. and Stöffler,G. (1988) *Nucleic Acids Res.* **16**, 815–832.
24. Laemmli,U.K. and Favre,M. (1973) *J. Mol. Biol.* **80**, 575–599.
25. Mitchell,P., Osswald,M., Schueler,D. and Brimacombe,R. (1990) *Nucleic Acids Res.* **18**, 4325–4333.
26. Kuechler,E., Steiner,G. and Barta,A. (1988) *Methods Enzymol.* **164**, 361–372.
27. Oβwald,M., Greuer,B. and Brimacombe,R. (1990) *Nucleic Acids Res.* **18**, 6755–6760.
28. Hagenbüchler,O., Santer,M., Steitz,J.A. and Mans,R.J. (1979) *Proc. Natl. Acad. Sci. USA* **76**, 3751–3754.
29. Youvan,D.C. and Hearst,J.E. (1979) *Proc. Natl. Acad. Sci. USA* **76**, 3751–3754.
30. Smith,J.E., Cooperman,B.S. and Mitchell,P. (1992) *Biochemistry* **31**, 10825–10834.
31. Abdurashidova,G.G., Tsvetkova,E.A. and Budowsky,E.I. (1991) *Nucleic Acids Res.* **19**, 1909–1915.

32. Lim,V., Venclovas,C., Spirin,A., Brimacombe,R., Mitchell,P. and Müller,F. (1992) *Nucleic Acids Res.* **20**, 2627–2637.
33. Ofengand,J., Ciesiolka,J., Denman,R. and Nurse,K. (1986) In Hardesty,B. and Kramer,G. (eds), *Structure, Function, and Genetics of Ribosomes*. Springer Verlag, New York and Heidelberg, pp. 473–494.
34. Gutell,R.R. and Fox,G.E. (1988) *Nucleic Acids Res.* **16**, r175–r269.
35. Cantor,C.R., Pellegrini,M. and Oen,H. (1974) In Nomura,M., Tissières,A. and Lengyel,P. (eds), *Ribosomes*. Cold Spring Harbor Laboratory Press, Cold Spring Harbor, pp. 573–585.